Journal of Engineering Research

Volume 6 | Issue 2 Article 6

2022

Interaction mechanism of Soil-ICB Grid

Islam Anas Elkorashi

Vol. 6, No. 2 – 2022 Journal of Engineering Research (ERJ)

Interaction Mechanism of Soil-ICB Grid

Islam Anas Elkorashi [1], Ahmed Farouk [2], Yousry Mowafy [3]

[1] PhD Candidate Faculty of Engineering, Al-Azhar University, Cairo, Egypt
Email: islam_elkorashi@f-eng.tanta.edu.eg

[2] Associate Prof., Structural Eng. Department, Faculty of Engineering, Tanta University, Tanta, Egypt
Email: drafarouk@f-eng.tanta.edu.eg

[3] Prof. of Geotechnical Engineering, Department of Civil Engineering, Al-Azhar University, Cairo, Egypt
Email: mowafy_2004@msn.com

***Abstract*- To understand the improved behaviour of the Isometric Cogged Biaxial Grid (ICBG), this research is devoted to evaluating the factors affecting the soil-grid interaction by separating the effect of friction, shear, and passive resistance between the soil and grid. Laboratory pull-out tests are carried out using two types of soil (sand and crushed limestone) reinforced by three different types of reinforcements, which are; a Solid Plate, a Biaxial Grid and the ICBG. It is found that the ICBG, which is a biaxial grid modified by distributing cogs on both sides of its ribs, added a new factor to the resistance mechanism, which is the interlocking with soil aggregates. This factor comprises about 34% of the resistance value. Moreover, the design of the ICBG results in greater improvement in passive resistance and introduces interlocking between the ribs and the aggregates which raises the final passive resistance by about 50% over the traditional Biaxial Grid. It is also found that for the ICBG passive resistance and the shear strength comprise about 47% of the pullout resistance, while in the case of using the Biaxial Grid the shear resistance has the demonstrative role with more than 70%.**

Keywords: **Biaxial Grid; Cogged Grid; Friction Force; ICB Grid; Soil-Grid interaction**

I. INTRODUCTION

Soil reinforcement is one of the most effective common soil improvement techniques. The reinforcement is carried out using tensile elements that are placed inside soils of weak strength to improve their stability and control deformation. Grids are among the most commonly used reinforcement, especially for granular soils. The grids are defined as "a planar polymeric product consisting of a regular dense network of parallel sets of ribs integrally connected at the junctions" [1]. The grids work in general by confining the soil particles increasing interlocking between the particles within the openings and resulting in a mechanically stabilized aggregate layer that exhibits an improved load-bearing performance.

The roughness at sand-geotextile interface resulted in improving interactions [18], while the geometry of a grid strongly influences the pullout behaviour of grids under small displacements [12]. Moreover, the static and dynamic behaviour of granular materials depends upon the shape of the grains [14].

The peak pullout resistance of the grids increases with the increase of the grid specimen size and this increment was more pronounced at high confining pressures [8]. The main factors affecting the soil-grid interaction are the friction, the interlocking of the soil through the apertures of the grid and the soil's particle size [13], [23] and [24]. In addition, the highest efficiency of Biaxial Grids occurs when the width of the grid's aperture is higher than 3.5 times the average particle's size of the soil [24]. It is worth noting that the recommendations and conclusions reported in the aforementioned studies were considered and applied to produce a novel cogged biaxial grid for improving the pull-out resistance of the reinforced soil [10] and [11]. The improvement would be gained by increasing the interface friction between the soil particles and the sine waveform cogs distributed on the ribs. The acronym of the proposed grid is "ICB Grid" as an abbreviation form of Isometric Cogged Biaxial Grid, which was suggested in previous research that presented a detailed description for the ICB Grid system [10] and [11].

The design of the ICBG depends on distributing small cubic cogs of 0.5×0.5×0.5cm on both surfaces of the biaxial grid elements as shown in figure 1. It may be interesting to mention that the efficiency of the ICBG relies basically on the idea of increasing the interlock between the soil aggregates and the Grid without decreasing the area of the openings. This change is believed to give a better performance of the ICBG than that of the traditional Biaxial Grid under pullout loading conditions.

Fig. 1: A photo showing the distribution of the cogs on the ribs of the ICBG

II. THEORETICAL BACKGROUND

Many researchers shed the light on the behaviour of the grids during the pullout tests and investigated the factors affecting the interaction between soil and grids during tests [5], [15], [19], [21], [22], [26] and [27]. The interaction mechanism of a soil-biaxial grid system is presented in

figure 2, showing that this mechanism can be divided into a primary and a secondary mechanism [27].

The secondary mechanism is due to friction at the soil-grid interface, whereas the primary mechanism comprises of three different components, which are;

i. The mechanical properties of the grid,
ii. The Interlock between the reinforcement and the soil is represented by the passive resistance between the soil aggregates and grid ribs, as well as the shear force between the soil located within the openings of the grid and the soil above and below the grid, and
iii. The confinement provided by the Grid openings.

Accordingly, the major parameters contributing to the mobilization of the primary mechanism are; the material properties of the grid, (i.e. tensile strength, elongation and creep), grid geometry and configuration, particle size and shape, and the soil density.

On the other hand, the frictional resistance mobilized between the grid and soil in the secondary mechanism is governed by the texture and shape of the particles, hardness of the aggregates, surface shape of the grid, grid material, and the relative stiffness between the grid and the soil aggregates.

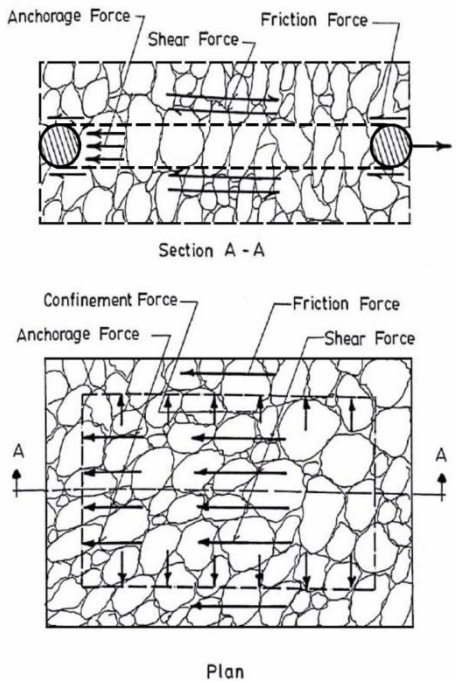

Fig. 2: Different forces resisting the pull-out load of the Biaxial Grid [27]

Finally, it should be mentioned that in case of perfect confinement, the soil particles within the openings must move with the grid, that is, there would be no relative movement between the confined aggregates and the grid during pull-out [27].

The main objective of this research is to investigate the influence of the aforementioned parameters on the overall performance of soil reinforcement systems and to quantify the resisting forces that dominate the soil-ICBG interaction mechanism. The interaction mechanism is studied in this paper for three different types of soil reinforcements, which are; a thin plate without openings, a biaxial grid, and an ICBG. In the preliminary studies, pull-out tests were conducted on different soil reinforcement systems and the results are used to analyze and quantify the aforementioned parameters.

III. EXPERIMENTAL PULL-OUT TESTS AND RESULTS

A series of pull-out tests were carried out on reinforced sand and another series was performed on a reinforced crushed limestone. Properties of the investigated materials are illustrated in table 1, and the particle-size distributions are shown in figure 3.

Table 1: Main characteristics of the tested materials

Soil	Sand	Crushed Limestone
Dry Density	16 (kN/m^3)	14 (kN/m^3)
Internal Friction Angle Φ	28°	42°
$D_{10\%}$	0.27 (mm)	5.2 (mm)
$D_{60\%}$	0.72 (mm)	8 (mm)
C_U	2.6	1.54

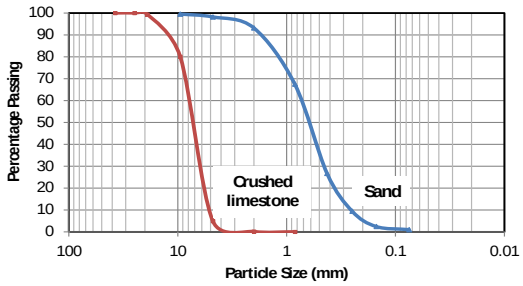

Fig. 3: Particles-size distribution of the investigated materials

Due to some manufacturing difficulties, the reinforcements used in this study were not made of polymers but steel 37. However, this agrees with the investigation done using a series of preliminary pull-out tests on steel meshes embedded in dense sand [16]. The physical and mechanical properties of steel 37 that were used in manufacturing the tested prototypes are illustrated in table 2.

Figure 4 illustrates the 3D geometries of parts of the studied reinforcements. All of these steel prototypes have the same overall length of 100 cm, the same width of 60 cm, and the same dominant thickness of 0.2 cm.

The pull-out tests were carried out according to the specifications of ASTM [3] with some modifications to suit the laboratory preparations that were mentioned in

previous researches [1], [2], [4], [9], [17], and [20]. Accordingly, a special pull-out testing tank and a loading frame were manufactured of mild steel to accommodate the tests of this study as illustrated in figure 5. The testing tank has an inner dimensional length, width and height of 100, 70 and 70 cm, respectively.

To compare the results, the Solid Plate and the ribs of both the Biaxial Geogrid and the ICBG have the same thickness of 0.20 cm. In addition, both the Biaxial Geogrid and the ICBG have the same aperture size of 4.5 × 4.5 cm, the same rib width of 0.50 cm, and the same total number of apertures of 240. It may be interesting to mention that the total number of the upper and lower cogs in the tested ICBG prototype is 2020 cogs.

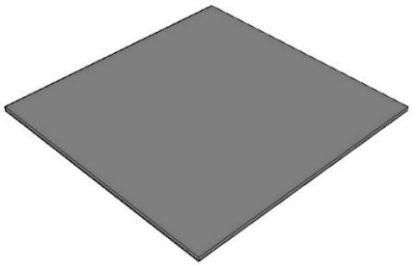

(a) The solid Plate

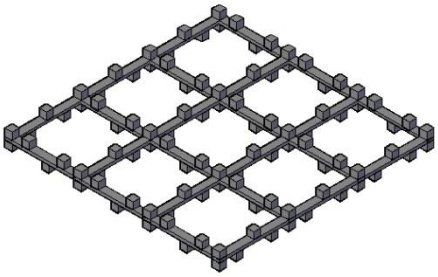

(b) The new ICBG

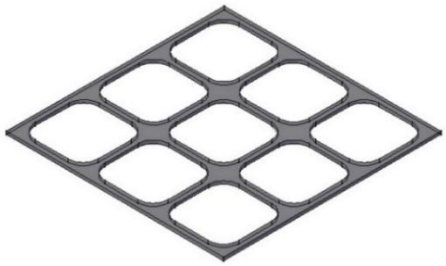

(c) The Biaxial Grid

Fig. 4: Schematic 3D geometries showing parts of the studied reinforcement prototypes

Table 2: Material properties of the tested prototypes (steel 37)

Density (γ)	**Elastic modulus** (E)	**Tensile strength** (R_m)	**Yield strength** (f_y)	**Shear modulus** (G)
78.5 (kN/m^3)	217 (Gpa)	340 - 470 (Mpa)	215 - 235 (Mpa)	75 - 80 (Gpa)

After completing the setup, each test was conducted at first by applying an external surcharge acting on the soil surface and then pulling out the soil reinforcement. tables (3), and 4 give a summary of the results and the calculated properties of the Pull-out Tests carried out on sand and crushed limestone respectively. In both tables, (σ_n) denotes the applied normal stresses in kN/m^2, (F) denotes the maximum pullout load in kN, and (τ_{ult}) denotes the corresponding ultimate shear strengths in kN/m^2.

Table 3: Main Summary of results of the pullout tests carried out on different types of reinforcement inside sand

(σ_n) kN/ m^2	Type of Ref.	(F) kN	Max. Disp. (mm)	(τ_{ult}) kN/m^2	Mode of failure
33.61	Solid Plate	19.62	22.35	16.35	slippage
	Biaxial Grid	58.86	26.11	49.05	slippage
	ICBG	90.74	23.6	75.62	arching
60.86	Solid Plate	22.1	20.98	18.42	slippage
	Biaxial Grid	93.20	24.11	77.66	slippage
	ICBG	142.25	25.56	118.54	slippage

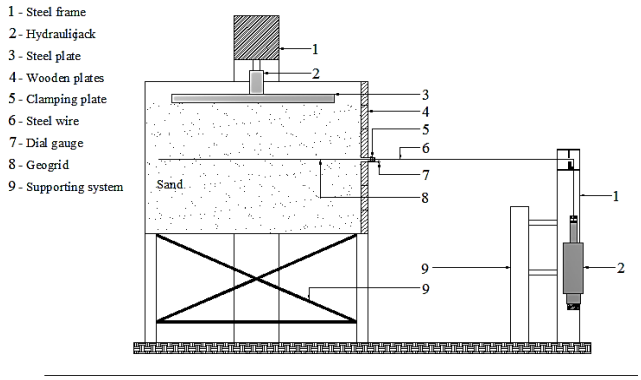

Fig. 5: Schematic representation showing the elevation view of the pull-out testing tank and the loading frame configuration (not to scale)

Table 4: Summary of results of the Pullout tests carried out on different types of reinforcement inside crushed limestone

(σ_n) kN/m^2	Type of Ref.	(F) kN	Max. Disp. (mm)	(τ_{ult}) kN/m^2	Mode of failure
14	Solid Plate	18.64	20.29	15.54	slippage
	Biaxial Grid	88.29	15.1	73.58	arching
	ICBG	98.1	13.06	81.75	arching
14.81	Solid Plate	19.62	23.65	16.35	slippage
	Biaxial Grid	93.2	13.39	77.67	arching
	ICBG	116.74	17.785	97.28	arching

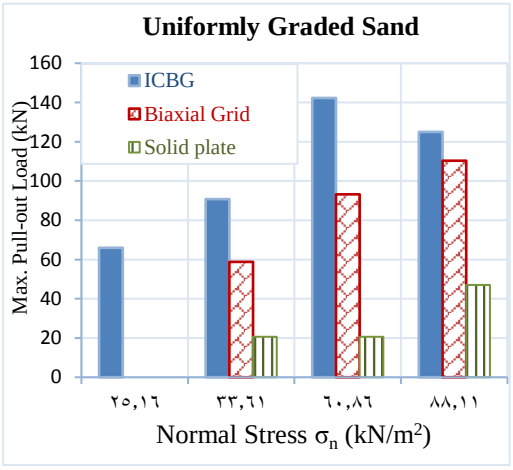

Fig. 6: Effect of the applied normal stress on the maximum pullout load for different types of reinforcement inside sand

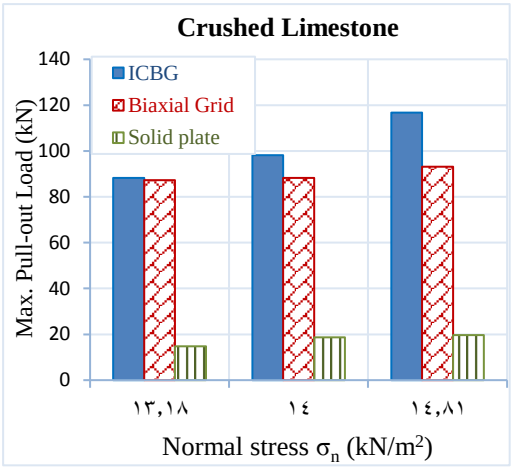

Fig. 7: Effect of the applied normal stress on the maximum pullout load for different types of reinforcements inside crushed limestone

Figures 6 and 7 illustrate relationships between the applied normal stress (σn) and the maximum pullout load (F) for sand and crushed limestone respectively. Both figures show that the pullout resistance of the ICBG is systematically higher than those obtained using the traditional Biaxial Grid for either sand or the crushed limestone. Moreover, it was noticed that the obtained results are the best representatives of the behaviour of grids since the relationships between the normal stresses (σ_n), and the corresponding ultimate shear strengths (τ_{ult}) are nearly linear as shown in figures 8 and 9, respectively [6]. Finally, it is worth noting that only the tests results which serve the main goal of this study are introduced [10] [11].

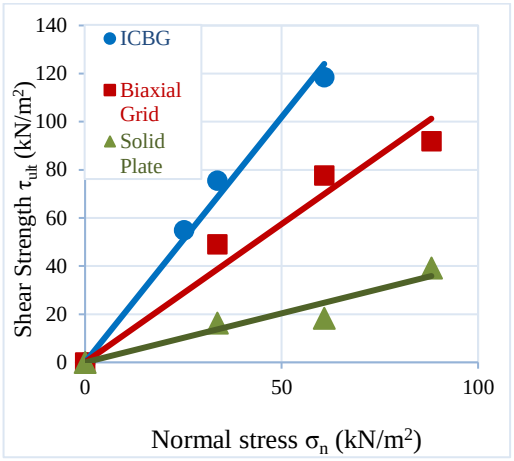

Fig. 8: Effect of using different types of reinforcement on the shear strength of the reinforced sand

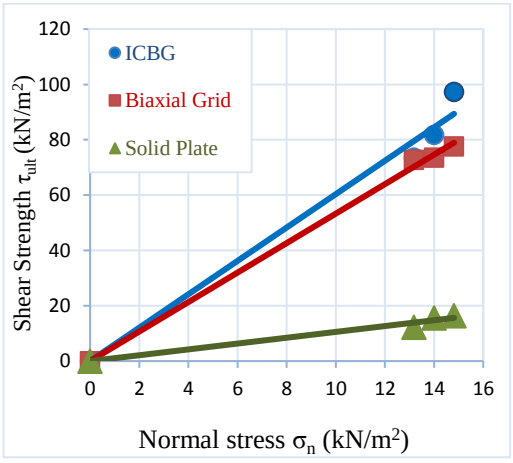

Fig. 9: Effect of using different types of reinforcement on the shear strength of the reinforced crushed limestone

IV.PREDICTION EQUATIONS OF PRIMARY AND SECONDARY RESISTANCE MECHANISM

To apply the theoretical resistance mechanism, the friction resistance, the passive resistance and the shear resistance should be separately quantified. The friction resistance (σ) between the soil and the steel can be defined using the test results of the steel Solid Plate as follows:

$$\sigma = \frac{F}{A_{steel}} \quad (1)$$

Where (σ) is the friction resistance in kN/m^2, (F) is the pullout load in kN, and (A_{steel}) is the summation of the upper and lower surface area of the steel plate in m^2.

Accordingly, the friction force (F_c) between soil and the upper and lower surfaces of any type of the tested steel prototypes (Solid Plate, Biaxial Grid, and ICBG) can be quantified as follows:

$$F_c = \sigma A_{steel} \quad (2)$$

In the case of the Biaxial Grid, the summation value of both the shear force (F_{sh}) and the passive force ($F_{pass(Biaxial)}$) can be calculated from equilibrium using the following equation:

$$(F_{sh} + F_{pass\,(Biaxial)}) = F_{Biaxial} - F_c \quad (3)$$

Where ($F_{Biaxial}$) is the pull-out load of the Biaxial Grid. Accordingly;

$$(F_{sh} + F_{pass\,(Biaxial)} + F_{pass\,(cogs)}) = F_{ICBG} - F_c \quad (4)$$

Where (F_{ICBG}) is the pull-out load of the ICBG.

From equation (3) and equation (4) the passive force generated by the cogs of ICBG can be quantified as:

$$F_{pass\,(cogs)} = F_{ICBG} - F_{Biaxial} \quad (5)$$

Now, the passive resistance in kN/m^2 generated by the cogs only ($\sigma_{pass\,(cogs)}$) can be quantified as follow:

$$\sigma_{pass\,(cogs)} = \frac{F_{pass\,(cogs)}}{A_{(cogs)}} \quad (6)$$

Where ($A_{(cogs)}$) is the area of the cogs facing the soil in the pull-out direction.

Since the passive resistance of the cogs ($\sigma_{pass\,(cogs)}$) and the passive resistance of the ribs are equal, then, the passive force (F_{pass}) generated by the thickness of the ribs in case of testing the Biaxial Grid can be quantified from the following equation:

$$F_{pass\,(Biaxial)} = \sigma_{pass\,(cogs)} A_{(pass)} \quad (7)$$

Consequently, the passive force generated by the ICBG can be quantified as:

$$F_{pass\,(ICB-GGR)} = F_{pass\,(Biaxial)} + F_{pass\,(cogs)} \quad (8)$$

Finally, the shear force (F_{sh}), for any grid type (Biaxial Grid or ICBG), can be estimated from:

$$F_{sh} = F - F_c - F_{pass} \quad (9)$$

Where (F) is either the pullout load of the Biaxial Grid ($F_{Biaxial}$) or the pullout load of the ICBG (F_{ICBG}) in kN depending on the type of reinforcement for which equation (9) is applied.

Figure 10 declares the application of the resistance mechanism on the new ICBG. It can be seen that for the ICBG, the forces in the right term of equation (3) shall be in equilibrium with the forces resisted by the grid shape in addition to the passive force generated by the protruded cogs ($F_{pass(cogs)}$).

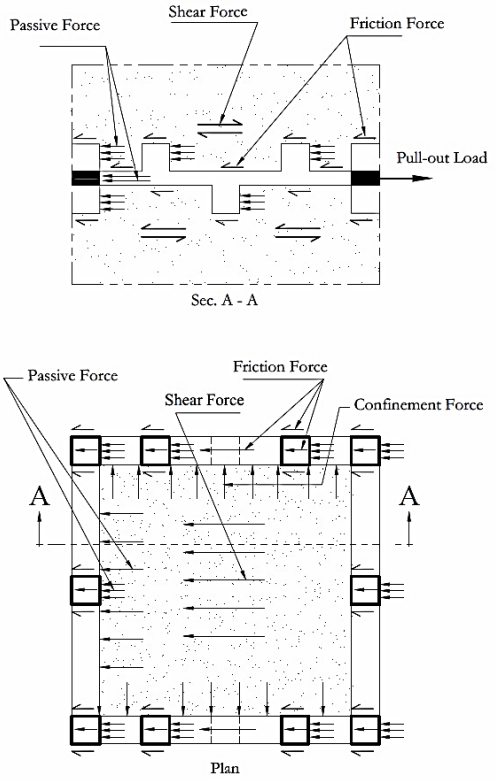

Fig. 10: The interaction mechanism of the new ICBG

V. ANALYSIS AND DISCUSSION OF COMPONENTS OF THE RESISTANCE MECHANISM

Different components of the resisting force acting on each of the tested prototypes can now be quantified using the values of the pull-out resistance obtained from the conducted pullout tests along with the aforementioned prediction equations. In the beginning, the areas to be used in the equations are calculated following the previously mentioned geometrical dimensions of each investigated prototype. Hence, the calculated areas are as follows:

$A_{steel\,(Solid\,Plate)} = 1.20\,m^2$

$A_{steel\,(Biaxial\,Geogrid)} = 0.264\,m^2$

$A_{steel\,(ICB-GGR)} = 2\,(A_{(ribs)} + A_{(cogs)}) = 0.329\,m^2$

From the theoretical explanation of the main components of the resistance mechanism, the following analysis depends on dissociating the results of the pullout tests to quantify each component of the resistance mechanism separately.

Tables 5 and 6 show summaries of the results obtained from the pull-out tests that were conducted on reinforced sands, while tables 7 and 8 summaries the results obtained from the pull-out tests performed on reinforced crushed limestone. The tables also represent the different calculated components of the resisting mechanism, which are the friction force (F_c) expressing the secondary resistance mechanism, as well as the shear force (F_{sh}) and the passive force (F_{pass}) which together represent the primary resistance mechanism. In the tables, the letter (q) denotes the external surcharge, (σ_n) denotes the normal stress acting on the grid, and (F) denotes the pull-out load measured in the tests.

Table 5: Summary of the results and the calculated forces of pullout tests carried out on different reinforcements embedded in sand

q (kN/m²)	σn (kN/m²)	Type of Ref.	F (kN)	σ (kN/m²)	Fc (kN)	Fpass (kN)	Fsh (kN)
27.25	33.61	Biaxial Grid	58.86	16.35	4.32	13.05	41.49
		ICBG	90.74	16.35	5.38	43.87	41.49
54.5	60.86	Biaxial Grid	93.195	18.42	4.86	20.26	68.075
		ICBG	142.245	18.42	6.06	68.11	68.075

Table 6: Percentages of the contribution of the primary and the secondary resisting forces of pull-out load for different reinforcements embedded in sand

σn (kN/m²)	Type of Ref.	% Fc	%Fpass	%Fsh
33.61	Biaxial Grid	7.34	22.17	70.49
	ICBG	5.93	48.35	45.72
60.86	Biaxial Grid	5.21	21.74	73.05
	ICBG	4.26	47.88	47.86

Table 7: Summary of the results of pullout tests carried out on different reinforcements embedded in crushed limestone and the calculated forces

q (kN/m²)	σn (kN/m²)	Type of Ref.	F (kN)	σ (kN/m²)	Fc (kN)	Fpass (kN)	Fsh (kN)
19.81	14	Biaxial Grid	88.29	15.54	4.1	3.73	80.46
		ICBG	98.1	15.54	5.11	12.53	80.46
10.63	14.81	Biaxial Grid	93.2	16.35	4.32	9.52	79.36
		ICBG	116.74	16.35	5.38	32	79.36

Table 8: Main Percentages of the contribution of the primary and the secondary resisting forces of pull-out load for different reinforcements embedded in crushed limestone

σn (kN/m²)	Type of Ref.	% Fc	%Fpass	% Fsh
14	Biaxial Grid	4.65	4.22	91.13
	ICBG	5.21	12.77	82.02
14.81	Biaxial Grid	4.64	10.21	85.15
	ICBG	4.61	27.41	67.98

VI.THE SECONDARY RESISTANCE MECHANISM

Quantifying the friction force (F_c) is the most appropriate start to analyze the pull-out resistance mechanism for the investigated reinforcements. As shown in figures 11 and 12 whether the soil is sand or crushed limestone and at any value of the applied normal stress (σ_n), the friction force (F_c) is the only resisting force in case of using the Solid Plate as a reinforcement.

The behaviour of granular materials under static or dynamic loads is dependent upon the shape of the grains, which encompasses all aspects of the external morphology of the particle, including form, roundness and surface texture [14]. This explains the constancy of percentages of (F_c) of the ICBG when reinforcing either sand or crushed limestone although the big difference between the values of the applied normal stress. This can be attributed to the fact that the interlock between the cogs of the ICBG and the aggregates compensates for the difference between the grains sizes in both cases. On the other hand, the effect of the grains' sizes on the values of the friction force (F_c) is noticeable in cases of testing either sand or crushed limestone reinforced with the Biaxial Grid although the value of this force is still relatively very small.

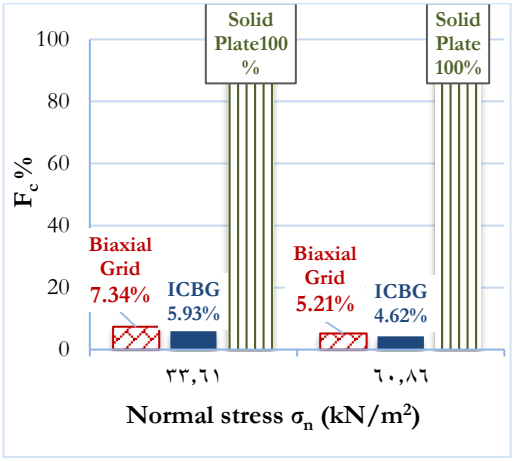

Fig. 11: Percentages of the friction force resistance (F_c) for different types of reinforcement embedded in sand

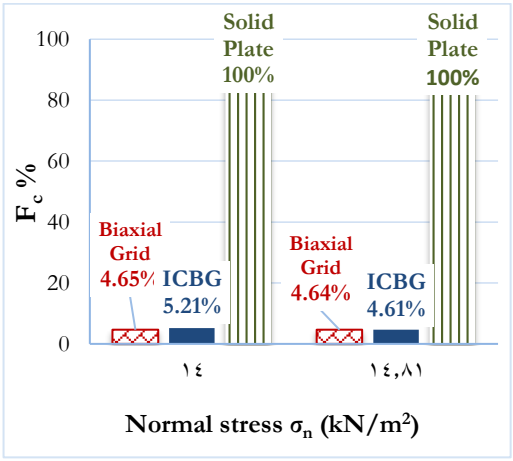

Fig. 12: Percentage of the friction force resistance (F_c) for different types of reinforcement embedded in crushed limestone

VII. THE PRIMARY RESISTANCE MECHANISM

Two main forces are constituting the primary resistance mechanism, which are the passive force (F_{pass}) and the shear force (F_{sh}). In the following subsections, percentages of the contribution of each of these forces in resisting the pullout load of the tested Biaxial Grid as well as of the tested ICBG, either embedded in sand or crushed limestone, are discussed in detail.

A. *The passive resisting force* (F_{pass})

Figures 13 and 14 hold comparisons for the sharing percentage of the passive force in resisting the pull-out load for reinforced sand and reinforced crushed limestone using either the Biaxial Grid or the ICBG. It can be seen that in the case of reinforcing sand with the Biaxial Grid, the

passive resisting force (F_{pass}) is nearly 20% of the total pull-out resisting force, while in the case of reinforcing crushed limestone also using the Biaxial Grid this percentage drops to about 4% which is almost the same percentage of the friction force (F_c) quantified at the same conditions.

Figure 13 clarifies that when reinforcing sand using the ICBG, the percentage of the (F_{pass}) reaches approximately 50% of the pullout load because of the existence of the cogs. This behaviour attributes the high peak pullout resistance of grids to the significant contribution of the passive resistance mobilized against the grid transverse members to the overall pullout capacity of the reinforcement [7].

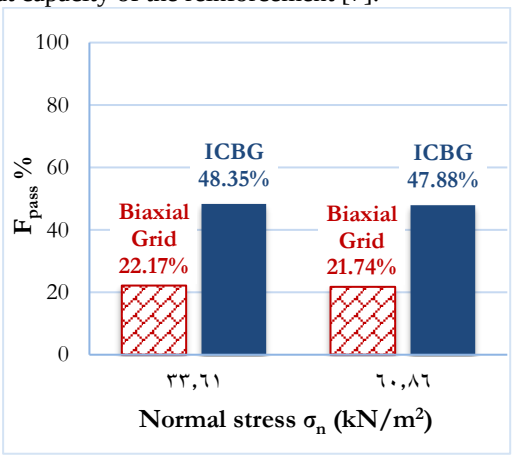

Fig. 13: Percentages of the passive force resistance (F_{pass}) of Grids embedded in sand

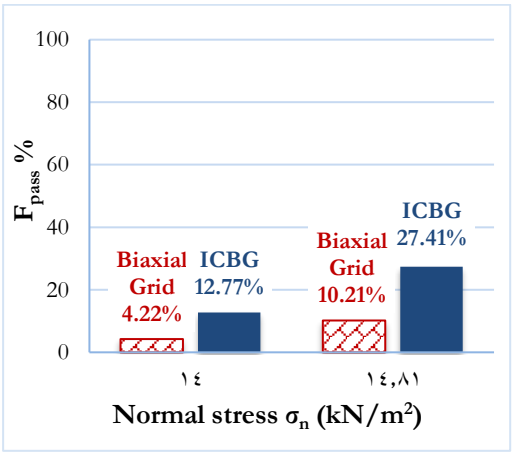

Fig. 14: Percentages of the passive force resistance (F_{pass}) of Grids embedded in crushed limestone

On the other hand, in the case of reinforcing crushed limestone with the ICBG, there is another factor that interferes to decrease the contribution percentage of the passive force (F_{pass}) to less than 30%. This interfering factor is the low value of the applied normal stress (σ_n), which is the major factor affecting the passive resisting force and, hence, affecting the efficiency and the benefit of the cogs. At this point, it should be cleared out that the resistance of the crushed limestone during the tests was high compared to the resistance of the sand under the same circumstances, and hence, there was no possibility to use higher values of the pullout load as the testing system was not designed to sustain such values.

B. The shear resisting force (F_{sh})

Because of the existence of the plain ribs in the Biaxial Grid, the shear force (F_{sh}) has the major share in the resisting mechanism with percentages that vary from 70% to nearly 90%, as shown in figures 15 and 16. It is worth noting that this trend was the same whether the Biaxial Grid is reinforcing sand or reinforcing the crushed limestone.

The same behaviour is almost noticed when using the ICBG to reinforce the crushed limestone, as the percentages of the shear resisting force (F_{sh}) is about 82% at an applied normal stress of 14.0 kN/m^2 and decreased to nearly 68% when the normal stress was raised to 14.8 kN/m^2 . This decrease in the shear resisting force as the normal stress increases is attributed to the resulting increase in the passive resistance due to the existence of the cogs. Contrary to this case, when the ICBG is used to reinforce sand; the shear force (F_{sh}) is only about 48%, which is nearly the same share as the passive force (F_{pass}) as shown in figure 13. Again, this behaviour also can be attributed to the high value of the applied normal stress, which in turn increases the passive resistance, leading to decreasing the share of the shearing resistance.

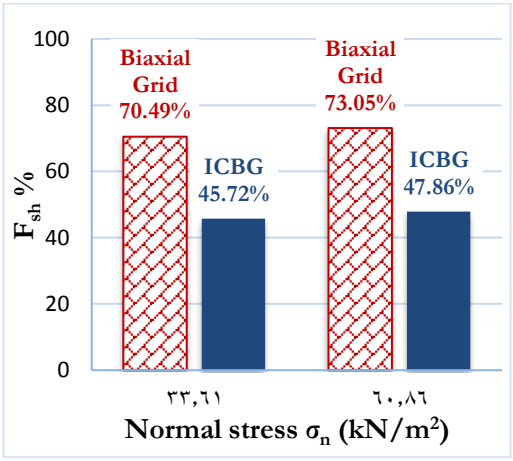

Fig. 15: Percentages of the shearing force resistance (F_{sh}) for Grids embedded in sand

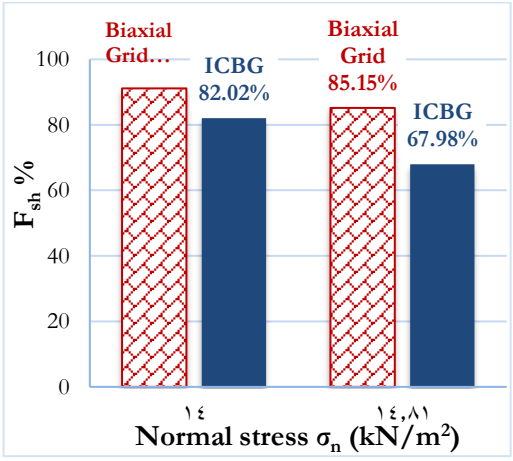

Fig. 16: Percentages of the shearing force resistance (F_{sh}) for Grids embedded in crushed limestone

VIII. EFFECT OF COGS ON THE PRIMARY RESISTANCE MECHANISM

Modifying the design of the conventional Biaxial Grid by adding cogs to construct the new ICBG, gives an approximately equal share to the main forces constituting the primary resistance mechanism, which are the passive force (F_{pass}) and the shear force (F_{sh}) in case of pulling the ICBG out of the sand. On the other hand, in the case of performing the test on crushed limestone, the share percentage of the shear force (F_{sh}) rises to be more than twice the share percentage of the passive force (F_{pass}) and that could be attributed to the relatively big particles' size of the crushed limestone besides the low value of the applied surcharge that constitutes the main factor affecting the passive resistance.

In general, as shown in figure 17, both the passive force (F_{pass}) and the shear force (F_{sh}), show a compatible behaviour for both investigated soils with a high improvement in the sharing percentage of the passive force (F_{pass}) in case of testing sand which could be attributed to the required applied surcharge that was higher than the applied surcharge in case of testing the crushed limestone. However, the comparison, which is presented in figure 17, clearly shows the effect of adding cogs to the grid on the primary resistance mechanism during pull-out tests.

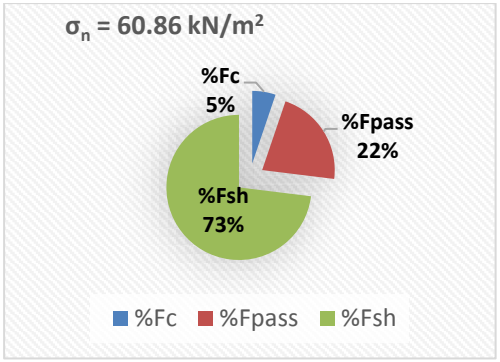

(a) Biaxial Grid pulled out from sand

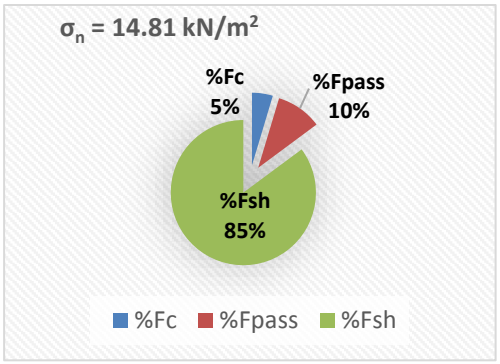

(b) Biaxial Grid pulled out from crushed limestone

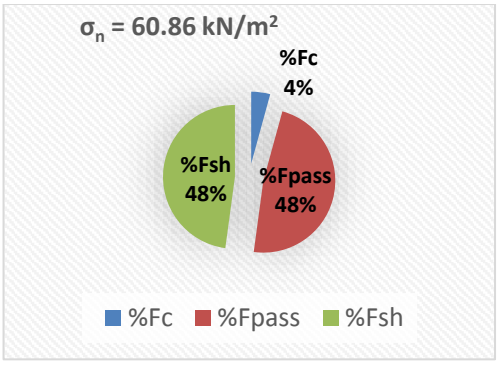

(c) ICBG pulled out from sand

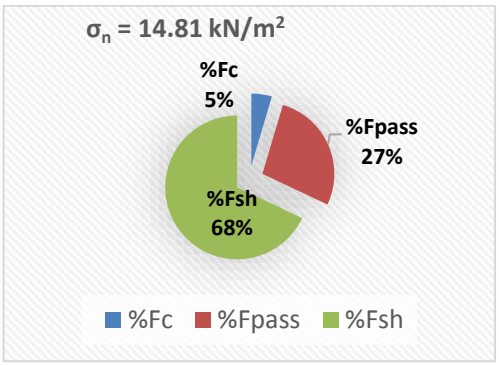

(d) ICBG pulled out from crushed limestone

Fig. 17: Comparisons between the contribution percentages of the resistance mechanism components for both the Biaxial Grid and the ICBG

IX. CONCLUSIONS

In the context of studying the improved performance of the newly innovated ICBG in the pull-out resistance, this study discussed both the primary and the secondary components of the resistance mechanism that affect the performance of the ICBG in comparison with the conventional Biaxial Grid. The main conclusions drawn from this study can be summarized as follows:

1. The percentages of the forces mobilized through the ribs of both the Biaxial Grid and the ICBG tend to increase with the increase of the applied normal stress as well as with the decrease of the size of used soil aggregates.

2. The cogs of the ICBG added a new factor to the resistance mechanism, which is the interlock between the ribs and the aggregates that share about 34% of the value of the total resistance.

3. The design of the new ICBG adds much more benefit to the passive resistance and introduces interlocking between the cogs and the soil particles, which raises the final passive resistance by about 50% over the Biaxial Grid.

4. As the secondary mechanism depends on the shape of the Grid, the cogs perform effectively in improving the whole interaction mechanism by increasing the generated passive resistance between the aggregates and the ICBG ribs and making a clear interlock between the grid and the soil.

5. The performance of the ICBG is better than the performance of the Biaxial Grid with the same type of soil under higher values of normal stress.

6. The share of interlock between the cubic cogs of the ICBG and the soil aggregates decreased by reducing the overburden pressure values in the case of reinforcing crushed limestone.

7. As revealed from the primary resistance mechanism analysis, the load mobilization criteria with the Biaxial Grid depends mainly on the interlock between soil aggregates, which may lead to a bad performance in the case of reinforcing poor types of soil.

8. The primary load mobilization mechanism of the ICBG shows a decrease in the share of soil aggregates interlock than the Biaxial Grid. This proves the efficiency of the use of the ICBG with the small soil particles that have poor resistance, which is the main aim of the innovative design of the new ICBG.

REFERENCES

1. A. Duszyńska and A. F. Bolt, "Pullout tests of geogrids embedded in non-cohesive soil," Archives of Hydroengineering and Environmental Mechanics, vol. 51, no. 2, pp. 135–147, 2004.
2. A.H. Abdel-rahman, M. A. Ibrahim, and A. K. Ashmawy, "Utilization of a Large-Scale Testing Apparatus in Investigating and Formulating the Soil/Geogrid Interface Characteristics in Reinforced Soils," Australian Journal of Basic and Applied Sciences, vol. 1, no. 4, pp. 415–430, 2007.
3. ASTM D6706-0101, "Standard Test Method for Measuring Geosynthetic Pullout Resistance in Soil," American Society for Testing and Materials (ASTM) International, vol. 1, no. Reapproved, pp. 1–8, 2013, doi: DOI: 10.1520/D6706-01R13.
4. C. W. Hsieh, G. H. Chen, and J. H. Wu, "The shear behavior obtained from the direct shear and pullout tests for different poor graded soil-geosynthetic systems," *Journal of GeoEngineering*, vol. 6, no. 1, pp. 15–26, 2011, doi: 10.6310/jog.2011.6(1).2.
5. D. T. Bergado, K. C. Macatol, N. U. Amin, J. C. Chai, M. C. Alfaro, and L. R. Anderson, "Interaction of lateritic soil and steel grid reinforcement," Canadian Geotechnical Journal, vol. 30, no. 2, pp. 376–384, 1993, doi: 10.1139/t93-032.
6. D. U. Infante, G. A. Martinez, P. Arrúa, and M. Eberhardt, "Behavior of geogrid reinforced sand under vertical load," International Journal of GEOMATE, vol. 10, no. 3, pp. 1862–1868, 2016, doi: 10.21660/2016.21.5168.
7. F. B. Ferreira, C. S. Vieira, and M. de L. Lopes, "Pullout Behavior of Different Geosynthetics—Influence of Soil Density and Moisture Content," Frontiers in Built Environment, vol. 6, no. February, pp. 1–13, 2020, doi: 10.3389/fbuil.2020.00012.
8. F.M. Nejad, J.C. Small (2005) Pullout behavior of geogrids. Iranian Journal of Science & Technology 29(B3): 301-310.
9. G. Cardile, M. Pisano, P. Recalcati, and N. Moraci, "A new apparatus for the study of pullout behaviour of soil-geosynthetic interfaces under sustained load over time," Geotextiles and Geomembranes, vol. 49, no. 6, pp. 1519–1528, 2021, doi: 10.1016/j.geotexmem.2021.07.001.
10. I. Anas, A. Farouk, M. B. El Sideek, A.-R. Hassan, and Y. Mowafy, "An Innovative Shape of Geogrid to increase Pull-Out Capacity," IOSR Journal of Mechanical and Civil Engineering, vol. 13, no. 04, pp. 72–79, Apr. 2016, doi: 10.9790/1684-1304017279.
11. I. Elkorashi, M. El Sideek, A. Hassan, Y. Mowafy, and A. Farouk, "Experimental and Numerical Study of the Isometric Cogged Biaxial Geogrid (Icb-Ggr)," Journal of Al-Azhar University Engineering Sector, vol. 15, no. 57, pp. 1052–1063, 2020, doi: 10.21608/auej.2020.120365.
12. J. Eun, R. Gupta, and J. G. Zornberg, "Effect of Geogrid Geometry on Interface Resistance in a Pullout Test," Mar. 2017, pp. 236–246, doi: 10.1061/9780784480472.025.
13. J. Giroud, "An assessment of the use of geogrids in unpaved roads and unpaved areas," on Polymer Geogrid Reinforcement. Identifying the …, 2009.
14. L. E. Vallejio, and L.F. Vesga, "ANALYSIS OF PARTICLE SHAPE USING FRACTALS," in *GeoFlorida 2010: Advanced in Analysis, Modeling & Design*, 2010, no. Gsp 199, pp. 2012–2021.
15. L. S. Calvarano, D. Gioffrè, G. Cardile, and N. Moraci, "A stress transfer model to predict the pullout resistance of extruded geogrids embedded in compacted granular soils," *10th International Conference on Geosynthetics, ICG 2014*, no. April 2016, 2014.
16. M. Loli, I. Georgiou, A. Tsatsis, R. Kourkoulis, and F. Gelagoti, "Pull-out testing of steel reinforced earth systems: Modelling in view of soil dilation and boundary effects," *Physical Modelling in Geotechnics*, no. July, pp. 1383–1387, 2018, doi: 10.1201/9780429438646-98.
17. M. Mosallanezhad, S. H. S. Taghavi, N. Hataf, and M. C. Alfaro, "Experimental and numerical studies of the performance of the new reinforcement system under pull-out conditions," Geotextiles and Geomembranes, vol. 44, no. 1, pp. 70–80, 2016, doi: 10.1016/j.geotexmem.2015.07.006.
18. M. R. Abdi and M. Safdari, "Studying the Effect of Roughness on Soil-Geotextile Interaction in Direct Shear Test," Journal of Engineering Geology, vol. 12, no. January, pp. 1–30, 2018.
19. N. Moraci, D. Cazzuffi, L. S. Calvarano, G. Cardile, D. Gioffrè, and P. Recalcati, "The influence of soil type on interface behavior under pullout conditions," *Geosynthetics*, vol. 32, no. 3, pp. 42–50, 2014.
20. O. A. Senoon, A-A.A. and Farghal, "Influence of the confinement, soil density, and anchorage length of reinforcement on soil geogrid interaction," 2003.
21. Palmeira, "Soil-Geosynthetics Interaction : Modelling and Analysis Mercer Lecture 2007-," no. January 2007, 2014.
22. N. Moraci and D. Gioffrè, "A simple method to evaluate the pullout resistance of extruded geogrids embedded in a compacted granular soil," Geotextiles and Geomembranes, vol. 24, no. 2, pp. 116–128, 2006, doi: 10.1016/j.geotexmem.2005.11.001.
23. R. D. Holtz and W. F. Lee, "WA-RD 532.1: Internal Stability Analyses of Geosynthetic Reinforced Retaining Walls.," Washington State Transportation Center (TRAC), no. January 2002, 2002.
24. R. M. Koerner, Design with Geosynthetics, 5th ed. New Jersey: Pearson Prentice Hall, 2005.
25. S. K. Shukla and J.-H. Yin, *Fundamentals of Geosynthetic Engineering*, Third 3rd. Taylor & Francis Group, London, UK, 2006.
26. W. Müller and W. Andreas, "Influence Of Rib Stiffness and Limited Long-Term Junction Strength on Geogrid Performance," 2019.
27. Y. Mowafy, "Analysis of Grid Reinforced Earth Structures," Carelton University, 1986.